

### Publication III

Minna Toivola, Lauri Peltokorpi, Janne Halme, and Peter Lund. 2007. Regenerative effects by temperature variations in dye-sensitized solar cells. *Solar Energy Materials & Solar Cells*, volume 91, number 18, pages 1733-1742.

© 2007 Elsevier Science

Reprinted with permission from Elsevier.

# Regenerative effects by temperature variations in dye-sensitized solar cells

Minna Toivola\*, Lauri Peltokorpi, Janne Halme, Peter Lund

*Department of Engineering Physics and Mathematics, Helsinki University of Technology, Laboratory of Advanced Energy Systems, P.O. Box 4100, FIN-02015 TKK, Finland*

Received 24 January 2007; accepted 28 May 2007  
Available online 17 July 2007

## Abstract

The effect of repeated temperature variations on the performance of both fresh and aged dye-sensitized solar cells with liquid and semi-solid electrolytes has been studied. The cell performance was characterized with *IV*-curves obtained at different cell operating temperatures and electrochemical impedance spectroscopy measurements before and after the temperature treatments. Consecutive temperature rampings of the aged cells did regenerate the cell function, so that the total efficiency drop over the observation period was on average 18%/unit less for the temperature-treated cells than for reference cells aged at constant temperature.

© 2007 Elsevier B.V. All rights reserved.

*Keywords:* Dye-sensitized solar cell; Temperature; Aging

## 1. Introduction

The dye-sensitized, nanostructured titanium dioxide solar cell (DSC) was first introduced in the early 1990's [1] and its low-cost materials, simple manufacturing methods and potential for high-throughput industrial mass production have gained remarkable worldwide research interest since then. Considerable progress has been made both in the cell efficiencies [2–4] and identification and development of new cell materials and manufacturing techniques. However, a lot of issues considering the long-term stability of the cells, which need to be clarified prior to commercial breakthrough of the technology, remain still open. Further analysis on the response of the cells to varying physical conditions during their aging, for example, temperature or air humidity, would also help to identify what kind of factors define and limit the cell performance in real-life end-user applications.

Depending on the operating environment of the DSCs (indoor/outdoor applications, placement of the modules and geographical location), their temperature can vary

from subzero values to near 100 °C [5,6]. As the cell's operation is based on repetitive chemical reaction cycles characterized by rate-determining kinetic constants, catalytic activity and charge transfer in various materials, temperature is likely to play a noticeable role on the cell's performance.

Compared to the other aspects in improving the DSC technology, the combined effect of temperature variations and aging to the cell behavior has been studied relatively little so far. For example, Petterson et al. [7,8] have studied the effect of operational conditions (illumination intensity, air humidity, temperature, short- or open-circuit operation) on the long-term stability of encapsulated DSC modules aimed for indoor applications. Their results showed that storage at temperatures under 50 °C does not affect the module performance but at higher temperatures cell degradation occurs mostly due to reduced open-circuit voltage. Sebastián et al. [9] have also reported similar temperature behavior for DSCs. Sommeling et al. [10] and Sastrawan et al. [11] have performed accelerated aging tests for DSCs, showing that even if storage at high (85 °C) temperatures results in decreased cell performance, the effect is partially reversible when the temperature is lowered again and the cells subjected to illumination.

\*Corresponding author. Tel.: +358 9 4513217; fax: +358 9 4513195.  
E-mail address: [minna.toivola@tkk.fi](mailto:minna.toivola@tkk.fi) (M. Toivola).

On the other hand, constant heating at 85 °C combined with full sun illumination leads to serious cell degradation [10]. Accelerated aging tests conducted by Hinsch et al. [12] indicate that thermal stress is one of the most critical factors affecting the long-term stability of the cells. They propose that cell degradation caused by aging in elevated temperatures ( $\geq 60$  °C) is very likely due to temperature-induced chemical changes in the electrolyte and that cell stability is strongly dependent e.g. on the chemical composition of the electrolyte and (water and oxygen) impermeability of the cell sealing material. Kern et al. [13] and Wang et al. [14] have used electrochemical impedance spectroscopy (EIS) to identify the internal cell processes responsible for the performance deterioration, and degradation mechanisms of the DSCs have also been studied by Macht et al. [15] and Junghänel et al. [16], though not directly as a function of temperature. Several factors were identified in Ref. [15], including the chemical instability of the electrolyte which manifested itself as loss of iodine ( $I_3^-$ ), a process triggered by water penetration into the cell and apparently favored by higher temperatures whereas in Ref. [16] the chemical bonding of the dye to the photoelectrode material appeared to be the most critical factor determining the long-term stability of the cells.

Snaith et al. [17] have investigated the dependence of the open-circuit voltage on light intensity, temperature and device thickness of solid-state DSCs, whereas Berginc et al. [18] have studied how the performance of DSCs filled with ionic liquid electrolyte is affected by the cell temperature, irradiance and iodine concentration in the electrolyte. Temperature dependence of various physical parameters of the cells, e.g. the electron quasi-Fermi level [19], electron diffusion coefficient [20], electron transport time [21] and conduction and mobility of the electrons in the nanostructured  $TiO_2$  [22] has also been addressed but not directly related to cell aging.

Degradation of the dye has been discussed e.g. in a review article by Tributsch [23] and by Grünwald et al. [24]. Greijer-Agrell et al. [25] have also showed that the chemical stability of the dye is strongly affected by temperature (detectable chemical changes start to occur when the cells are subjected to temperatures of 125–200 °C). More advanced dye materials can, however, improve the temperature (and long-term) stability of the cells, as has been demonstrated by Wang et al. [26,27].

Temperature is likely to affect the kinetic rate constants of the DSC reactions (e.g. recombination, dye adsorption/desorption and catalytic reduction of tri-iodide on the counter electrode) and ionic mobility, diffusion and conductivity in the electrolyte as well [28].

The objective of this research was to investigate how repeated temperature variations affect the performance of both fresh and aged dye solar cells filled with liquid or semi-solid iodine electrolyte and prepared from as-received, non-purified starting materials resembling cleanliness levels typical of hypothetical industrial conditions. This viewpoint is valid considering upscaling of the cell

manufacturing from clean laboratory conditions to industrial production facilities such as sheet steel production lines, where laboratory-type purity standards are not necessarily met. For example, stainless steel is a potential low-cost and flexible substrate material for the DSC, and coating the cell directly onto metallic building materials as a part of their manufacturing process has already gained commercial interest [29–33].

For performance characterization, the cell operating temperature was varied in ramps 20 → 40 → 70 → 40 → 20 °C and *IV*-curves were measured in all aforementioned temperatures for fresh, 10–12 days aged and ca. one month (29 days) aged cells. To complement the *IV*-curve data and to gain more detailed information about the electrical behavior of the cell components, EIS measurements were also employed before and after every temperature ramping. Temperature increase might have a regenerative effect on the performance of aged cells, especially those filled with semi-solid electrolytes [34] which was also verified in this study.

The consecutive temperature rampings during aging slowed down the decrease of the cell efficiencies, which was caused mostly by degradation of the short-circuit current as a function of time. However, the currents were partly regenerated in every temperature treatment, which resulted in a lower overall degradation rate in the cell performance. On average, the ratio of the 1-month-aged and temperature-treated cell efficiency to the efficiency of the fresh cells was 18%/unit higher than the same ratio obtained with the reference cells aged at constant (room) temperature in the dark. EIS measurements also showed that after the temperature ramping, charge-transfer resistance on the counterelectrode—electrolyte interface was lower and the electron lifetimes in the  $TiO_2$  film longer than before that, both in fresh and aged cells. Thus it can be deduced that the temperature treatment had a refreshing effect on the cell function; not permanent, but it still indicates that instead of having a detrimental effect on the long-term performance of the cells, repeatedly and regularly varying temperature is more likely to be beneficial to it. In general, the best performance was obtained at 40 °C and the temperature behavior was very similar for all cell types.

## 2. Experimental

### 2.1. Photoelectrodes

$TiO_2$  photoelectrodes were prepared both on FTO glass (Pilkington TEC-15, thickness 2.5 mm, sheet resistance 15  $\Omega$ /sq., supplied by Hartford Glass Company, Inc.) and ITO-PET plastic (NV-CT-CH-1S-M-7, thickness ca. 0.2 mm, sheet resistance 60  $\Omega$ /sq., supplied by Bekaert Specialty Films, Inc.) substrates. Before use, the substrates were cut to 16 mm × 20 mm pieces and washed first with water and mild detergent, after which the cleaning was finished in an ultrasonic bath 3 min first in ethanol and then in acetone.  $TiO_2$  was distributed through a 4 mm × 8 mm rectangular mask made of 60  $\mu$ m thick Scotch tape with a

doctor-blading method using either commercial TiO<sub>2</sub> paste (Sustainable Technologies International) or 20wt% ethanol suspension of TiO<sub>2</sub> nanoparticles (P25, Degussa) as the precursor. On ITO–PET, only the latter was used due to the post-treatment temperature limitations of the plastic. Two layers of TiO<sub>2</sub> precursors were spread and in the case of P25 suspension, mild compression (125–250 kg/cm<sup>2</sup>) in a hydraulic press was applied on every layer to improve the interparticle adherence and contact to the substrate. Electrodes made of the commercial paste were dried on a hot plate at 100 °C before the second layer was spread and finally, all glass photoelectrodes were sintered in an oven at 500 °C for 30 min. For plastic photoelectrodes, only compression was used as the post-treatment. An electronic film thickness measurement device (Heidenhain Digitaler Messtaster MT12; resolution 0.1 μm) was used to determine the thickness of the TiO<sub>2</sub> films which was ca. 10 μm for all electrodes. Finally, the electrodes were sensitized by soaking them overnight in 0.32 mM absolute ethanol solution of the N-719 dye (*cis*-bis(isothiocyanato)bis(2,2'-bipyridyl-4,4'-dicarboxylato)-ruthenium(II) bis-tetrabutylammonium, Solaronix SA). After the sensitization, the electrode films were rinsed with and stored in absolute ethanol.

## 2.2. Electrolytes

Two types of electrolytes were used: liquid electrolyte which consisted of 0.5 M LiI, 0.05 M I<sub>2</sub> and 0.5 M 4-*tert*-butylpyridine (TBP) in 3-methoxypropionitrile (MePRN) and semisolid electrolyte made of the former by gelatinizing it with 5wt% of PVDF–HFP (polyvinylidene fluoride–hexafluoropropylene), a method described in the literature [26].

## 2.3. Counterelectrodes

Platinized glass counterelectrodes (16 mm × 20 mm, Pilkington TEC-15) were employed in all cells. Platinization was done with the standard thermal method, as described previously [32].

## 2.4. Cell assembly

The electrodes were sealed together on a hot plate (100 °C) using 50 μm thick Surlyn<sup>®</sup> 1702 film as a spacer

and sealant, after which the electrolyte was filled into the cells through small holes drilled on the counterelectrode substrates. Holes were blocked with a thin slice of a microscope cover glass and a Surlyn<sup>®</sup> film and finally, current collector contacts made of aluminum tape and conducting silver paint applied on the edges of the electrodes. Table 1 summarizes the cell types prepared for this study.

## 2.5. Measurements

*IV*-curve measurements were performed with a custom-built solar simulator consisting of ten 150 W halogen lamps as the radiation source, a temperature-controlled measurement plate, and a calibrated monocrystalline silicon reference cell with which the lamps could be adjusted to provide the standard light intensity of 100 mW/cm<sup>2</sup>. The spectral mismatch factor of the simulator, defined with the reference cell and the measured spectral irradiance of the halogen lamps [35,36] was used to make the curves correspond with the standard AM1.5G equivalent illumination. *IV*-curves were measured first at 20 °C, then at 40 and 70 °C after which the temperature was lowered and curves obtained again at 40 and 20 °C. For fresh cells, only the upward sweep of the temperature ramp (20 → 40 → 70 °C) was used. Due to the varying room temperature, air circulation and the nature of the temperature control system (Peltier elements) the accuracy of the temperatures was ca. ±2 °C. A few cells of each series were chosen as reference cells which were let to age at constant (room) temperature in the dark. Both *IV*-curves and EIS spectra of the reference cells were measured on the same days as the temperature-treated cells. Before measurements, cells were let to stabilize at a given temperature for ca. 10 min. EIS spectra were recorded with Zahner Elektrik's IM6 Impedance Measurement Unit operated with Thales software using a red LED (wavelength 640 nm) as the radiation source. The spectra were obtained with 10 mV voltage amplitude in the 100 mHz–100 kHz frequency range at open-circuit voltage, at room temperature (22–24 °C) before and after the temperature ramp measurements in the solar simulator. To provide repeatable measurement conditions, the LED and the cells were placed in a darkened box to block out external light. ZPlot/ZView<sup>®</sup>

Table 1  
Cell types

Cell type	PE substrate	TiO <sub>2</sub> -precursor	Electrolyte	CE
G-STI-L	Glass	Commercial titania paste	Liquid	Pt glass
G-STI-G	Glass	Commercial titania paste	Gel	Pt glass
G-P25-L	Glass	TiO <sub>2</sub> -nanoparticle-ethanol suspension	Liquid	Pt glass
G-P25-G	Glass	TiO <sub>2</sub> -nanoparticle-ethanol suspension	Gel	Pt glass
P-P25-L	Plastic	TiO <sub>2</sub> -nanoparticle-ethanol suspension	Liquid	Pt glass
P-P25-G	Plastic	TiO <sub>2</sub> -nanoparticle-ethanol suspension	Gel	Pt glass

PE, photoelectrode; CE, counterelectrode.

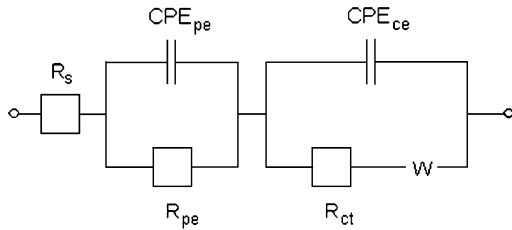


Fig. 1. Equivalent circuit used for the EIS spectra fits.  $R_s$  = series resistance of the cell;  $R_{pe}$  = photoelectrode resistance (electron diffusion in the  $\text{TiO}_2$  film and recombination on the  $\text{TiO}_2$ -dye-electrolyte interface);  $\text{CPE}_{pe}$  = constant phase element describing the Helmholtz layer capacitance on the  $\text{TiO}_2$  film surface;  $R_{ct}$  = charge-transfer resistance on the counterelectrode–electrolyte interface;  $\text{CPE}_{ce}$  = constant phase element describing the counterelectrode capacitance;  $W$  = Warburg element associated with the diffusion in the electrolyte. Constant phase elements were used instead of pure capacitances because they describe better a realistic, uneven and inhomogenous electrode surface [37].

software from Scribner, Inc. was used for equivalent circuit fits of the EIS spectra. Fig. 1 describes the model circuit used in the fits. All measurements described above were performed for fresh, 10–12 days and ca. 1-month (29 days)-aged cells. Between the measurements, the cells were stored in the dark and at room temperature to provide controlled aging conditions.

### 3. Results and discussion

#### 3.1. Differences between the cell types

Neither aging, nor temperature behavior or the regenerative effects caused by the temperature treatments varied much between the cell types. P25-ethanol suspension gave slightly better cell efficiencies than the commercial titania paste, whereas gel electrolyte resulted in lower cell performance (than liquid) which is easily explained with the gel's poorer penetration into the pores of the  $\text{TiO}_2$  layer. The lowest performances (<1% efficiencies) were obtained with the plastic photoelectrode cells. This indicates poor interparticle connections and adhesion to the substrate, which is why the results concerning these cell types are not discussed further in this paper. For future reference, another  $\text{TiO}_2$  deposition method than doctor blading should be selected for plastic.

#### 3.2. *IV*-curves

##### 3.2.1. The effect of temperature on fresh cells

Table 2 presents the operating parameters and Fig. 2 examples of the *IV*-curves of fresh cells measured at different temperatures. Increasing the temperature from 20 to 40 °C resulted in a slight gain in short-circuit currents ( $I_{sc}$ ) and a small drop in open-circuit voltages ( $V_{oc}$ ) for all cell types. When the temperature was raised further to 70 °C, a radical decrease was noticed both in  $I_{sc}$  and  $V_{oc}$ . Fill factors (FF), on the other hand, were higher at increased temperatures due to the slopes of the *IV*-curves

Table 2

Average cell parameters (four cells per type) at different temperatures, measured right after cell preparation

Cell type	Temperature (°C)	$I_{sc}$ (mA/cm <sup>2</sup> )	$V_{oc}$ (V)	FF (%)	$\eta$ (%)
G-STI-L	20	12.1	0.62	54	4.0
	40	12.5	0.60	59	4.4
	70	10.8	0.54	61	3.6
G-STI-G	20	8.6	0.59	60	3.0
	40	8.8	0.57	62	3.1
	70	7.1	0.51	63	2.3
G-P25-L	20	11.6	0.65	59	4.4
	40	11.5	0.62	61	4.4
	70	10.1	0.56	62	3.5
G-P25-G	20	10.5	0.59	55	3.4
	40	10.6	0.57	58	3.5
	70	9.3	0.51	60	2.9

Standard deviations of the independent results are not listed in the table, but their values fell in the range  $\pm 0.01$  V for  $V_{oc}$ ,  $\pm 0.3$ – $1.0$  mA/cm<sup>2</sup> for  $I_{sc}$ ,  $\pm 1$ – $3\%$  for FF and  $\pm 0$ – $0.3\%$  for  $\eta$ .

becoming steeper around the open circuit voltage. The total cell resistance ( $R_{tot}$ ) contributes to the reciprocal slope of the *IV*-curve around  $V_{oc}$ , and even if the values of the individual components of  $R_{tot}$  (e.g. photoelectrode resistance, charge-transfer resistance on the counter electrode, solution resistance of the electrolyte and sheet resistance of the substrates) cannot be obtained from the *IV* data alone it can be assumed that the temperature increase has a reducing effect at least on some of them, for example, the charge-transfer resistance on the counterelectrode, which is related to the activity of the Pt catalyst on it. Energy conversion efficiencies ( $\eta$ ) were generally the highest at 40 °C, due to the gains in  $I_{sc}$  and FF.

The slight increase in the  $I_{sc}$  at 40 °C could be explained with more efficient electron diffusion in the  $\text{TiO}_2$  film. According to the trapping/detrapping model for the electron transport in the nanocrystalline  $\text{TiO}_2$ , Peter et al. [20] have shown that the apparent electron diffusion coefficient increases with temperature as more electrons are released from trap states to the conduction band. On the other hand, the rate constant for the recombination reaction for the conduction band electrons with the  $I_3^-$  in the electrolyte also increases with temperature [19]. This has a tendency to decrease both  $I_{sc}$  and  $V_{oc}$ , but this effect did not seem to be dominant yet at 40 °C, because the general behavior of the  $I_{sc}$  was the opposite. Thus it can be assumed that if the temperature increase is modest, the more efficient diffusion of the electrons in the  $\text{TiO}_2$  may compensate the higher recombination rate.

Temperature-induced changes in the conduction band electron density indicate linear decrease in the open circuit-voltage with temperature [19,20]. This was held true with good accuracy for the cells in this study; ( $dV_{oc}/dT$ ) averaged over all cell series being  $-1.65 \pm 0.1$  mV/K. In addition to Ref.[19], Dürr et al. [38] have derived a linear dependency for  $V_{oc}$  as a function of  $T$  as well, and have also confirmed the direct relation between the

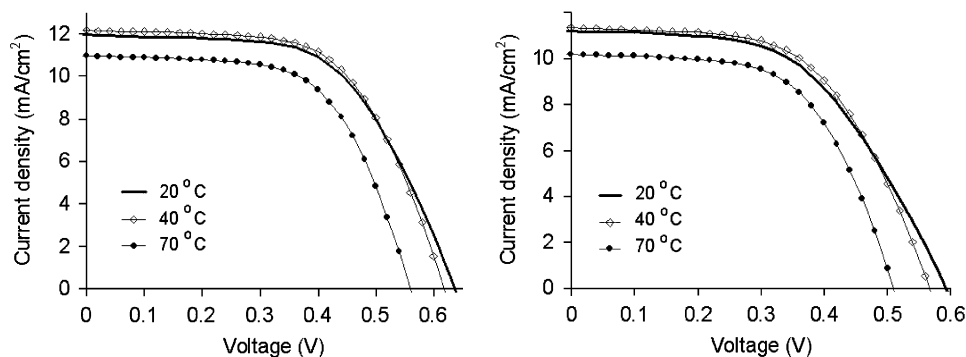


Fig. 2. Examples of the  $IV$ -curves of the cell types G-P25-L (left) and G-P25-G (right) at different temperatures, measured with  $100\text{ mW/cm}^2$  AM1.5G equivalent light intensity. Cell active area  $0.32\text{ cm}^2$ .

recombination rate and the rate of the  $V_{oc}$  decrease with temperature.

The lowest efficiencies for all cell types were recorded at  $70^\circ\text{C}$ , indicating more disadvantageous, most likely activation-triggered effects starting to take place at the higher temperatures. Even if increased recombination did not seem to have a crucial effect on the cell operation yet at  $40^\circ\text{C}$ , the situation might be different when the temperature is raised above that. Another possible explanation for the radical drop both in  $I_{sc}$  and  $V_{oc}$  at  $70^\circ\text{C}$  could be reversible re-adjustment of the chemical composition of the  $\text{TiO}_2$  surface, i.e. equilibrium between the dye, electrolyte additives and impurities in it (reversibility of these effects is discussed later in Section 3.2.2).

### 3.2.2. Aging behavior of the cells and the effect of temperature treatment

The degradation in the cell performance as a function of time appeared as reduced short-circuit current, whereas the open-circuit voltage remained almost the same over the observation period. However, temperature treatment led to improvement in the aged cell performance (consistent e.g. with Sommeling et al. [10]). Table 3 presents the average parameters of fresh, 10–12 days and ca. 1-month-aged cells before and after the temperature treatment, Fig. 3 examples of the  $IV$ -curves measured on days 10–12 and Fig. 4 the cell efficiencies as a function of time.

Some possible reasons for the decrease in the  $I_{sc}$  over time are dye degradation (caused e.g. by impurities such as water in the electrolyte) or desorption [14], dissolution of platinum from the counter electrode [39,40] and changes in the  $\text{TiO}_2$  film structure and/or in the electrolyte. If platinum is detached from the counterelectrode, it could diffuse to the photoelectrode and act there as a recombination center. This would show as increased  $R_{ct}$  on the counterelectrode and also as reduced  $V_{oc}$ . Indeed, a slight decline can be observed in the  $V_{oc}$  as a function of time, especially for the reference cells (charge-transfer properties on the counterelectrode are discussed in more detail in Section 3.3.3). However, as other causes than platinum attachment on the  $\text{TiO}_2$  can also increase recombination

over time, the platinum dissolution from the counter-electrode needs to be verified separately. The  $V_{oc}$  of the aged cells was, in any case, more sensitive to temperature increase than the  $V_{oc}$  of the fresh cells. The  $(dV_{oc}/dT)$  were  $-1.83 \pm 0.2\text{ mV/K}$  for the 10–12-days-aged cells and  $-1.95 \pm 0.1\text{ mV/K}$  for the 29-days-aged cells which, if the charge generation rate remained constant, would indicate increasing recombination with time [19,38]. In general, platinum dissolution as well as dye desorption are irreversible effects, and if these happened on a large scale, no regeneration in the cell performance can be achieved even with the temperature treatment.

Disadvantageous changes in the  $\text{TiO}_2$  film structure include loosening of the interparticle connections or the contact between the film and the substrate (unlikely for the sintered films, though), which would increase the overall resistance of the cell. Electrolyte leakage or evaporation has caused cell deterioration in some cases, [15] but the sealing method used in this study eliminates this problem.

Unwanted side reactions in the electrolyte or reactions of the electrolyte species and/or  $\text{TiO}_2$  with possible impurities present in the cell (water, oxygen) can also lower the cell performance over time. In this study, the most probable explanation for the deteriorating short-circuit currents and efficiencies are indeed impurities in the electrolyte (and possible dye degradation caused by them). As all chemicals were of non-ultrapure quality, used as-received and stored in normal room conditions instead of oxygen, and water vapor-free atmosphere, the purity of the electrolyte was probably lower than if careful pretreatment such as distillation or re-crystallization of its ingredients had been performed. For example, LiI is hygroscopic and water molecules can be transported into the cell with it, especially if the electrolyte is prepared during high relative humidity.

As can be seen from Table 3, the refreshing effect caused by the temperature treatment on aged cells was mostly due to increased short-circuit current. During the downward sweep of the ramp, when the temperature was lowered from  $70^\circ\text{C}$ , the current set on higher levels at 40 and  $20^\circ\text{C}$  than what it had reached during the upward sweep, despite its radical drop at  $70^\circ\text{C}$ . In most cases this resulted in still

Table 3

Average performance parameters of fresh, aged and reference cells on different measurement days (four temperature treated and four reference cells per type)

Cell type	Day #	Before/after temperature treatment	$I_{sc}$ (mA/cm <sup>2</sup> )	$V_{oc}$ (V)	FF (%)	$\eta$ (%)
G-STI-L	1	Before	12.1	0.62	54	4.0
		After	–	–	–	–
		Reference	12.2	0.62	57	4.3
	12	Before	8.3	0.60	44	2.2
		After	12.0	0.62	44	3.3
		Reference	9.1	0.61	38	2.1
	29	Before	9.7	0.61	47	2.8
		After	11.1	0.63	48	3.3
		Reference	7.9	0.60	43	2.0
G-STI-G	1	Before	8.6	0.59	60	3.0
		After	–	–	–	–
		Reference	10.3	0.58	58	3.4
	12	Before	6.8	0.58	62	2.4
		After	7.8	0.60	62	2.9
		Reference	7.2	0.57	60	2.5
	29	Before	5.9	0.59	62	2.2
		After	6.7	0.61	63	2.6
		Reference	6.5	0.57	61	2.3
G-P25-L	1	Before	11.6	0.65	59	4.4
		After	–	–	–	–
		Reference	11.8	0.64	56	4.2
	10	Before	9.4	0.64	60	3.6
		After	10.4	0.67	60	4.1
		Reference	9.8	0.62	56	3.3
	29	Before	7.8	0.65	60	3.0
		After	8.5	0.67	61	3.4
		Reference	7.8	0.62	57	2.8
G-P25-G	1	Before	10.5	0.59	55	3.4
		After	–	–	–	–
		Reference	10.3	0.59	57	3.4
	10	Before	8.7	0.59	56	2.9
		After	9.9	0.60	57	3.3
		Reference	8.1	0.58	58	2.7
	29	Before	7.1	0.59	57	2.4
		After	7.9	0.61	58	2.8
		Reference	6.6	0.58	60	2.3

Standard deviations of independent results the same as in Table 2.

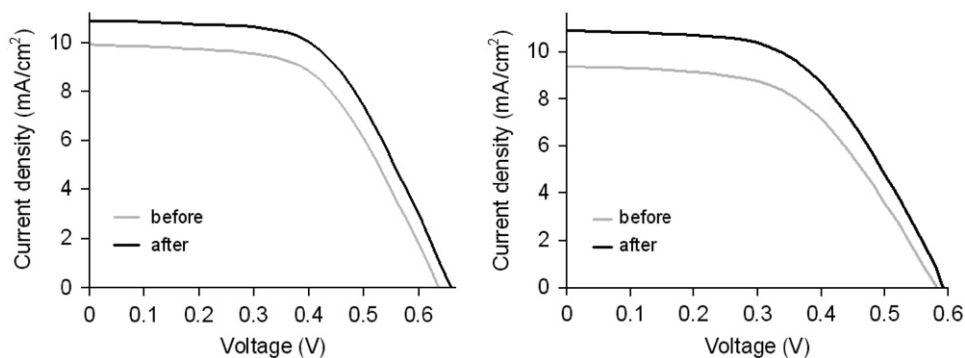


Fig. 3. Examples of the  $IV$ -curves on days 10–12, before and after the temperature treatments for the cell types G-P25-L (left) and G-P25-G (right), measured with 100 mW/cm<sup>2</sup> AM1.5G equivalent light intensity. Cell active area 0.32 cm<sup>2</sup>.

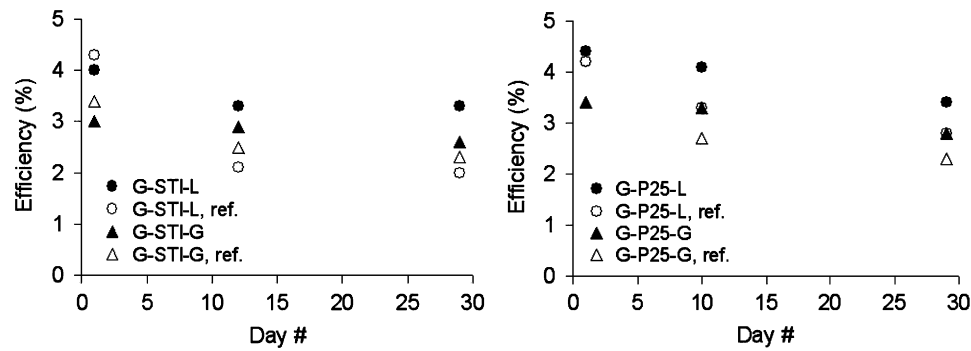


Fig. 4. The average cell efficiencies as a function of time, both temperature treated and reference cells. For temperature treated cells, efficiencies obtained after the temperature rampings are presented (cf. Table 3).

Table 4  
Cell efficiency ratios

Cell type	$\eta_2/\eta_1$ , temperature treated cells (%)	$\eta_2/\eta_1$ , reference cells (%)	$\eta_2/\eta_1$ , temperature treated— $\eta_2/\eta_1$ , reference cells (%-unit)
G-STI-L	83	50	33
G-STI-G	87	77	10
G-P25-L	77	64	13
G-P25-G	82	68	14

$\eta_1$  = initial cell efficiency,  $\eta_2$  = cell efficiency on day 29, after the last temperature treatment.

higher  $I_{sc}$  on the next consecutive measurement day than the level onto which the reference cell  $I_{sc}$  had decreased. Slight improvement could be detected also in fill factors and open-circuit voltages. In general, the regenerative effect that the temperature ramping had on the short-circuit currents made the average overall efficiency drop over the observation period ca. 18%/unit smaller for the temperature-treated cells, in comparison with the reference cells. Table 4 presents the ratios of the original cell efficiencies ( $\eta_1$ ) to those of the 29-days-aged cells ( $\eta_2$ ), measured after the last temperature ramping. Corresponding values for the reference cells are also listed.

In general, the results described above indicate the temperature behavior of the cells is at least partly controlled by reversible, activation-triggered physicochemical processes. Exact identification of these processes and their activation energies was beyond the scope of this research, but based on the results and those obtained in previous studies [8–14] it can be claimed that the maximum temperature for the satisfactory operation and long-term stability of the conventional, liquid/semi-solid iodine electrolyte DSC is in the range 50–60 °C.

In the future, the cell stability should be observed over a longer time period, with shorter temperature ramping intervals to mimic more closely the temperature variation caused by natural lighting cycles and also for cells aged under illumination similar to realistic operating conditions.

### 3.3. EIS measurements

#### 3.3.1. General trends in the EIS data

Three arcs in the Nyquist plots and two imaginary impedance peaks in the Bode plots could be observed for all cells (Figs. 5 and 6). The high-frequency peak (kHz range) can be associated with the charge transfer on the counterelectrode ( $R_{ct}$ – $CPE_{ce}$  in Fig. 1) and the middle frequency peak (ca. 10 Hz) with the photoelectrode impedance, generally characterized by the transport (diffusion) resistance of the electrons in the  $TiO_2$  film, recombination resistance of the electrons with the electrolyte species and the capacitance of the electrode ( $R_{pe}$ – $CPE_{pe}$  in Fig. 1) [13,14,41].  $R_{ct}$  and  $R_{pe}$  can be obtained from the Nyquist plots as the diameters of the high and middle frequency arcs, respectively, and the electron lifetime in the  $TiO_2$  film ( $\tau_{el}$ ) can be approximated from the frequency ( $f$ ) of the photoelectrode's imaginary impedance peak's minimum [13]:

$$\tau_{el} \approx \frac{1}{2\pi f}. \quad (1)$$

Because the impedance arcs of the photo- and counterelectrode partially overlapped in the Nyquist plots information on the transport resistance could not be directly extracted from the data. For this reason the photoelectrode impedance was fitted with a lumped RC-circuit instead of a transmission line model [41,42], in this paper.

The half visible arc in the low-frequency range of the Nyquist plots is due to the diffusion in the electrolyte [13,14,41]. For the cells in this study it was almost completely masked by the photoelectrode impedance, which is why it was left off the equivalent circuit fits as well.

#### 3.3.2. Photoelectrode impedance

For all cells, both temperature treated and reference ones,  $R_{pe}$  increased with time. Recombination increased also with time, deduced from the shorter electron lifetimes in the aged  $TiO_2$  films; consistent with the larger ( $dV_{oc}/dT$ ) measured with the aged cells and also with previously published results [13,14]. For the fresh cells, the  $R_{pe}$  were slightly larger also after the temperature treatment

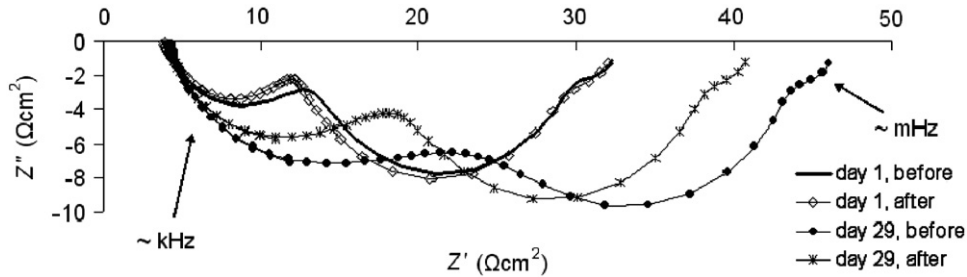


Fig. 5. Typical Nyquist plots, fresh and 29-days-aged cells, before and after temperature treatments. Cell type G-P25-G. Continuous lines are the respective fits.  $Z'$  = real impedance;  $Z''$  = imaginary impedance.

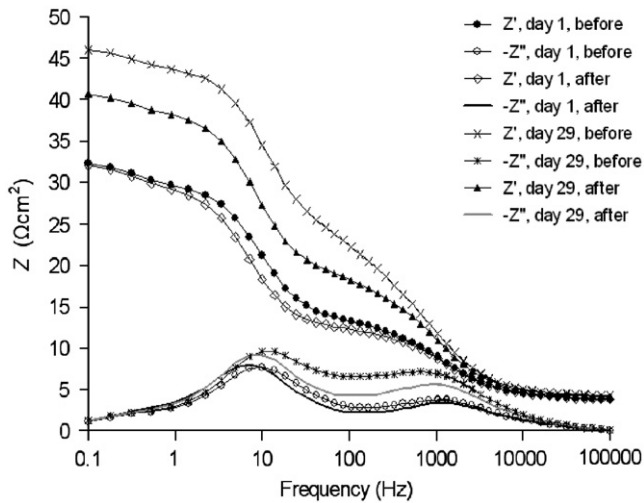


Fig. 6. Typical Bode plots, fresh and 29-days-aged cells, before and after temperature treatments. Cell type G-P25-G. Continuous lines are the respective fits.

(in agreement with Refs. [41,42], where increase with temperature is predicted for the electron transport resistance in the  $\text{TiO}_2$  film), whereas for the aged cells the behavior was generally the opposite. However, both for the fresh and aged cells the electron lifetimes were longer after the temperature treatments, to the extent that in some cases the values obtained after the last temperature ramping on day 29 were still on the same level or even larger than what had been measured from the fresh cells before the first ramping on day 1. This indicates that the temperature treatment had a beneficial effect on the recombination suppressing properties of the  $\text{TiO}_2$ -dye-electrolyte interface, i.e. the chemical composition of and equilibrium between the adsorbents on the  $\text{TiO}_2$  surface. For the reference cells, only steady decrease in  $\tau_{\text{el}}$  with time was observed.

The  $\tau_{\text{el}}$  can also be expressed as the time constant of the  $RC$ -circuit describing the photoelectrode (or, the recombination time constant)

$$\tau_{\text{el}} = R_{\text{pe}} C_{\text{pe}}. \quad (2)$$

Based on Eq. (2) increase in  $C_{\text{pe}}$  could result in larger  $\tau_{\text{el}}$ , even if  $R_{\text{pe}}$  decreased. Indeed, the photoelectrode capaci-

ties were larger after every temperature ramping, and when the  $\tau_{\text{el}}$  were calculated from these values using Eq. (2) the result was their increase even in the case of decreased  $R_{\text{pe}}$ .

When making assumptions based on the  $C_{\text{pe}}$  values their voltage dependence should also be noted. The changes in the open-circuit voltages with time and temperature in this study could affect the photoelectrode capacitances as well, which is why the  $V_{\text{oc}}$  values recorded during the EIS measurements should also be used to make detailed conclusions about the origins of the  $C_{\text{pe}}$  changes. The identification of the exact reason for the behavior of  $C_{\text{pe}}$  with time and temperature was not the purpose of this study, but changing chemical composition of the Helmholtz layer on the  $\text{TiO}_2$  surface, i.e. concentrations of the electrolyte additives (e.g. TBP) and/or possible electrolyte impurities in it may induce shifts in the  $\text{TiO}_2$  conduction band energy level position and affect the capacitances [41,42] (a reason that could partially explain also the radical drop in the cell efficiencies at  $70^\circ\text{C}$ , as discussed in Section 3.2.1).

To exactly identify the temperature-induced changes in the charge transport, the EIS spectra should be measured as a function of temperature too. We have performed this kind of measurement as well, both for fresh and aged cells, and their results will be discussed in another paper (in preparation).

### 3.3.3. Counterelectrode impedance

Because the same counterelectrode type was employed in all cells, the behavior of  $R_{\text{ct}}$  was also similar for all cell types. Charge-transfer resistance on the counter-electrode increased with time, indicating deteriorating electrode quality. However, temperature treatment refreshed the counterelectrode performance, i.e. decreased its charge-transfer resistance quite noticeably both for the fresh and aged cells. These results, along with those obtained for the  $R_{\text{pe}}$ , are consistent with the  $IV$ -curve measurements, where the slopes of the curves around the  $V_{\text{oc}}$  became steeper in higher temperatures, indicating smaller total resistance of the cell. They also agree with [14], where 2 days of thermal aging at  $80^\circ\text{C}$  was noticed to improve the counterelectrode performance (possibly due to activation of the Pt catalyst layer or better contact between it and the electrolyte).

Table 5  
Typical values of  $R_{pe}$ ,  $R_{ct}$  and  $\tau_e$ , before and after the temperature treatments

Cell type	Day #	Before/after temperature treatment	$R_{pe}$ ( $\Omega\text{cm}^2$ )	$R_{ct}$ ( $\Omega\text{cm}^2$ )	$\tau_e$ (ms)
G-STI-L	1	Before	17.1	6.9	29
		After	19.6	6.4	40
		Reference	17.9	9.2	25
	12	Before	20.9	10.3	25
		After	18.8	9.0	32
		Reference	20.5	11.7	18
	29	Before	24.1	11.8	20
		After	20.8	10.0	28
		Reference	23.7	11.4	15
G-STI-G	1	Before	21.6	9.2	15
		After	23.1	8.5	18
		Reference	23.0	10.8	16
	12	Before	32.3	15.7	8
		After	29.2	11.7	11
		Reference	31.2	16.6	10
	29	Before	38.9	23.0	8
		After	36.7	16.4	10
		Reference	36.0	23.6	10
G-P25-L	1	Before	15.4	5.4	21
		After	17.1	6.5	22
		Reference	15.9	4.4	25
	10	Before	19.8	10.9	17
		After	20.7	9.3	23
		Reference	17.8	7.2	20
	29	Before	22.3	15.5	14
		After	21.6	13.8	18
		Reference	19.8	9.4	17
G-P25-G	1	Before	17.1	9.5	18
		After	17.9	8.4	24
		Reference	17.0	7.3	18
	10	Before	19.5	14.5	15
		After	17.7	10.9	20
		Reference	20.1	9.9	12
	29	Before	22.2	18.6	14
		After	20.4	14.6	19
		Reference	24.2	11.9	10

Reference cell values are also listed.

Because the EIS results in this study were obtained after the cells had cooled down back to room temperature and kept there for a few hours, the regenerating effect that the temperature ramping had on the counterelectrode function seems to have at least some permanence and very likely plays a part in the observed slower overall deterioration rate for the temperature-treated cells.

Figs. 5 and 6 present typical EIS behavior for fresh and aged cells, and Table 5 lists some typical values of  $R_{pe}$ ,  $R_{ct}$  and  $\tau_e$  (calculated with Eq. (2)), before and after the temperature treatment. Series resistances (in the

Nyquist plot the distance between zero and the smallest value of the real impedance) fell in the range 10–13  $\Omega$  for all cells and they stayed almost constant over the observation period.

#### 4. Conclusions

We have studied the effects of temperature variations on the performance of both fresh and aged dye-sensitized solar cells filled with either liquid or semi-solid iodine electrolytes. Regenerative effect caused by consecutive temperature rampings on the aged cell performance has been demonstrated. Temperature and aging behavior were very similar for all cell types in this study, including best performance at 40 °C, a radical drop both in  $I_{sc}$  and  $V_{oc}$  at 70 °C and the cell degradation with time being caused mostly by the degenerating short-circuit current.

The efficiency drop at the highest temperatures was reversible, indicating that the cell function is at least partly controlled by activation-triggered physicochemical processes. When the aged cells were subjected to temperature ramping and, despite their low performance at 70 °C, the currents set on higher levels during the downward sweep of the ramp than what they had reached when the temperature was increased in its upward sweep, and compared with the reference cells, they were on this higher level still on the next consecutive measurement day. The electron lifetimes in the  $\text{TiO}_2$  film were also longer after the temperature treatment, indicating the treatment had a beneficial effect on the recombination-suppressing properties of the  $\text{TiO}_2$ -dye-electrolyte interface.

From the slopes of the  $IV$ -curves around the  $V_{oc}$  and from the EIS measurements, it could be detected that the temperature treatment lowered the total resistance of the cells. Especially the charge-transfer resistance on the counterelectrode stayed on this lower level even after the cells had cooled down back to room temperature and were kept there for a few hours.

Thus it can be summarized that the temperature treatments had a refreshing effect on the cell function, to the extent that the overall drop in the cell efficiencies over the observation period was on average 18%/unit smaller for the temperature-treated cells when compared with the reference cells that were let to age in constant temperature. From the EIS data and the behavior of  $(dV_{oc}/dT)$  as a function of time, it could also be verified that increased recombination and deteriorating counterelectrode quality were some of the reasons for the degradation of the cell performance over time. In general, based on the observations in this research and those obtained previously in other studies, it can be said that the maximum temperature for the satisfactory long-term operation of the DSCs is around 50–60 °C, and that repeatedly and regularly varying temperature is more likely beneficial to the aged cell performance, taken that the cells are not subjected to detrimentally high temperatures for very long periods of time.

## Acknowledgment

Financial support from the National Technology Agency of Finland (Tekes) is gratefully acknowledged.

## References

- [1] B. O'Regan, M. Grätzel, *Nature* 353 (1991) 737.
- [2] M. Grätzel, *Curr. Appl. Phys.* 6S1 (2006) e2.
- [3] M.K. Nazeeruddin, P. Pechy, T. Renouard, S.M. Zakeeruddin, R. Humphry-Baker, P. Comte, P. Liska, L. Cevey, E. Costa, V. Shklover, L. Spiccia, G.B. Deacon, C.A. Bignozzi, M. Grätzel, *J. Am. Chem. Soc.* 123 (2001) 1613.
- [4] M.K. Nazeeruddin, T. Bessho, L. Cevey, S. Ito, C. Klein, F. De Angelis, S. Fantacci, P. Comte, P. Liska, H. Imai, M. Grätzel, *J. Photochem. Photobiol. A* 185 (2007) 331.
- [5] K. Jyrkäs, R. Sipilä, Improvements in Weatherability Testing of Coil Coatings, Conference Transcript for ECCA General Meeting, Brussels, Belgium, 1998.
- [6] C. Sjöström, Service Life Analysis of Organic Coatings on Sheet Metal Façade Claddings, Royal Institute of Technology, Sweden, 1990.
- [7] H. Pettersson, T. Gruszecki, *Sol. Energy Mater. Sol. Cells* 70 (2001) 203.
- [8] H. Pettersson, T. Gruszecki, L.-H. Johansson, P. Johander, *Sol. Energy Mater. Sol. Cells* 77 (2003) 405.
- [9] P.J. Sebastián, A. Olea, J. Campos, J.A. Toledo, S.A. Gamboa, *Sol. Energy Mater. Sol. Cells* 81 (2004) 349.
- [10] P.M. Sommeling, M. Späth, H.J.P. Smit, N.J. Bakker, J.M. Kroon, *J. Photochem. Photobiol. A* 164 (2004) 137.
- [11] R. Sastrawan, J. Beier, U. Belledin, S. Hemming, A. Hinsch, R. Kern, C. Vetter, F.M. Petrat, A. Prodi-Schwab, P. Lechner, W. Hoffmann, *Prog. Photovolt.: Res. Appl.* 14 (2006) 697.
- [12] A. Hinsch, J.M. Kroon, R. Kern, I. Uhlendorf, J. Holzbock, A. Meyer, J. Ferber, *Prog. Photovolt.: Res. Appl.* 9 (2001) 425.
- [13] R. Kern, R. Sastrawan, J. Ferber, R. Stangl, J. Luther, *Electrochim. Acta* 47 (2002) 4213.
- [14] Q. Wang, J.-E. Moser, M. Grätzel, *J. Phys. Chem. B* 109 (2005) 14945.
- [15] B. Macht, M. Turrión, A. Barkschat, P. Salvador, K. Ellmer, H. Tributsch, *Sol. Energy Mater. Sol. Cells* 73 (2002) 163.
- [16] M. Junghänel, H. Tributsch, *C. R. Chimie.* 9 (2006) 652.
- [17] H.J. Snath, L. Schmidt-Mende, M. Grätzel, *Phys. Rev. B* 74 (2006) 045306.
- [18] M. Berginc, U. Opara Krašovec, M. Jankovec, M. Topič, *Sol. Energy Mater. Sol. Cells*, published online 28 March 2007.
- [19] K. Lobato, L.M. Peter, *J. Phys. Chem. B* 110 (2006) 21920.
- [20] L.M. Peter, A.B. Walker, G. Boschloo, A. Hagfeldt, *J. Phys. Chem. B* 110 (2006) 13694.
- [21] G. Boschloo, A. Hagfeldt, *J. Phys. Chem. B* 109 (2005) 12093.
- [22] H. Greijer-Agrell, G. Boschloo, A. Hagfeldt, *J. Phys. Chem. B* 108 (2004) 12388.
- [23] H. Tributsch, *Coordin. Chem. Rev.* 248 (2004) 1511.
- [24] R. Grünwald, H. Tributsch, *J. Phys. Chem. B* 101 (1997) 2564.
- [25] H. Greijer-Agrell, J. Lindgren, A. Hagfeldt, *Sol. Energy* 75 (2003) 169.
- [26] P. Wang, S.M. Zakeeruddin, M. Grätzel, *J. Fluorine Chem.* 125 (2004) 1241.
- [27] P. Wang, S.M. Zakeeruddin, J.E. Moser, M.K. Nazeeruddin, T. Sekiguchi, M. Grätzel, *Nat. Mater.* 2 (2003) 402.
- [28] P.W. Atkins, *Physical Chemistry*, fifth ed, 1994.
- [29] T. Ma, X. Fang, M. Akiyama, K. Inoue, H. Noma, E. Abe, *J. Electroanal. Chem.* 574 (2004) 77.
- [30] X. Fang, T. Ma, M. Akiyama, G. Guan, S. Tsunematsu, E. Abe, *Thin Solid Films* 472 (2005) 242.
- [31] M. Kang, N.-G. Park, K. Ryu, S. Chang, K.-J. Kim, *Sol. Energy Mater. Sol. Cells* 90 (2006) 574.
- [32] M. Toivola, F. Ahlskog, P. Lund, *Sol. Energy Mater. Sol. Cells* 90 (2006) 2881.
- [33] <<http://www.dyesol.com>>, accessed 5 April 2007.
- [34] K. Miettunen, Quasi-Solid Electrolyte in Dye-sensitized Solar Cells Deposited on Plastic and Stainless Steel: Literature Review and Preliminary Tests, Helsinki University of Technology, Finland, 2006, unpublished.
- [35] E. Luque, S. Hegedus, *Handbook of Photovoltaic Science and Engineering*, Wiley, Chichester, 2003.
- [36] J. Nelson, *The Physics of Solar Cells*, Imperial College Press, London, 2003.
- [37] J.R. Macdonald, *Impedance Spectroscopy*, Wiley, 1987.
- [38] M. Dürr, A. Yasuda, G. Nelles, *Appl. Phys. Lett.* 89 (2006) 061110.
- [39] E. Olsen, G. Hagen, S.E. Lindquist, *Sol. Energy Mater. Sol. Cells* 63 (2000) 267.
- [40] N. Papageorgiou, W.F. Maier, M. Grätzel, *J. Electrochem. Soc.* 144 (1997) 876.
- [41] F. Fabregat-Santiago, J. Bisquert, G. Garcia-Belmonte, G. Boschloo, A. Hagfeldt, *Sol. Energy Mater. Sol. Cells* 87 (2005) 117.
- [42] Q. Wang, S. Ito, M. Grätzel, F. Fabregat-Santiago, I. Mora-Seró, J. Bisquert, T. Bessho, H. Imai, *J. Phys. Chem. B*, published online 30 November 2006.